

# Tissue Engineering of a Periodontal Ligament–Alveolar Bone Graft Construct

Ai Mei Chou, BSc<sup>1</sup>/Varawan Sae-Lim, DDS<sup>2</sup>/Dietmar W. Hutmacher, PhD, MBA<sup>3,4</sup>/Tit Meng Lim, PhD<sup>1</sup>

**Purpose:** This paper reports on a 2-phase study of a novel membrane-scaffold graft construct, its ability to support periodontal ligament fibroblast (PDLF) and alveolar osteoblast (AO) growth *in vitro*, and its use for tissue engineering a PDL-AO interface *in vivo*. **Materials and Methods:** Human PDLFs were seeded onto perforated poly( $\epsilon$ -caprolactone) membranes ( $n = 30$ ) at 78,000 cells/cm<sup>2</sup>; human AOs were seeded on poly( $\epsilon$ -caprolactone) scaffolds ( $n = 30$ ) with fibrin glue at 625,000 cells/cm<sup>3</sup>. Cell attachment, morphology, viability, and metabolic activity were monitored for 3 weeks *in vitro*. Subsequently, cell-seeded membrane-scaffold constructs (experimental group,  $n = 9$ ) and nonseeded constructs (control group,  $n = 4$ ) assembled with fibrin glue were implanted subcutaneously into 7 athymic mice for 4 weeks. **Results:** PDLFs formed confluent layers on membranes, whereas AOs produced mineralized matrices within scaffolds upon osteoinduction *in vitro*. Well-vascularized tissue formation was observed after implantation. Integration at the membrane-scaffold interface was enhanced in the experimental group. Type I collagen, type III collagen, fibronectin, and vitronectin were found adjacent to membranes and within constructs. Bone sialoprotein expression and bone formation were undetectable. **Discussion:** Membrane perforation and scaffold porosity facilitated tissue integration and vascularization at the construct-recipient site. However, the interaction between PDLF and AO could have interfered with osteogenesis at the interface of soft and mineralizing tissues. **Conclusions:** Both matrices supported PDLF and AO attachment and proliferation *in vitro*. The membrane-scaffold construct facilitated tissue growth and vascularization while providing strength and form *in vivo*. INT J ORAL MAXILLOFAC IMPLANTS 2006;21:526–534

**Key words:** alveolar osteoblasts, graft construct, human periodontal ligament fibroblasts, poly( $\epsilon$ -caprolactone)

The presence of an intact periodontium, consisting of gingiva, periodontal ligament, cementum, and alveolar bone, is crucial for establishing a stable

bone-tooth interface. Thus, the regeneration of periodontal tissues lost to inflammatory processes related to either dental injuries<sup>1</sup> or periodontal diseases<sup>2</sup> is considered the ultimate aim in tooth retention.<sup>3</sup> Many therapeutic approaches, including the use of guided tissue regeneration membranes with or without bone grafts or substitutes, have failed to achieve predictable results<sup>4</sup> because of the complexity of the regenerative process at the soft tissue–hard tissue interface.<sup>2</sup> It was postulated that the provision of a prefabricated 3-dimensional structure with the appropriate cells or inductive molecules would be a viable regenerative strategy.<sup>4</sup>

Transplantation of periodontal scaffold-cell constructs has been previously reported. Investigations have included the implantation of human periodontal ligament fibroblasts (PDLFs) on collagen scaffolds into Sprague-Dawley rats,<sup>5</sup> of human cementum-derived cells on hydroxyapatite/tricalcium phosphate ceramic into immunodeficient mice,<sup>6</sup> and of human gingival autograft using hyaluronic acid scaffolds.<sup>7</sup> Recently, autologous PDL cells seeded onto a collagen sponge were used to regenerate cementum

<sup>1</sup>Department of Biological Sciences, National University of Singapore, Singapore.

<sup>2</sup>Associate Professor, Department of Restorative Dentistry, National University of Singapore, Singapore.

<sup>3</sup>Associate Professor, Division of Bioengineering, National University of Singapore, Singapore.

<sup>4</sup>Associate Professor, Department of Orthopaedic Surgery, National University of Singapore, Singapore.

**Correspondence to:** A/P Varawan Sae-Lim, Department of Restorative Dentistry, Faculty of Dentistry, National University of Singapore, 5 Lower Kent Ridge Road, Singapore 119074. Fax: +65 6 7732603. E-mail: rsdsvl@nus.edu.sg

The abstract of this article was presented at Symposium on Tissue Engineering Science: Critical Elements in the Research and Development Continuum, Aegean Conferences, 19–23 May 2002, Greece, and at the 7th National University Hospital–National University of Singapore (NUH-NUS) Annual Scientific Meeting, 16–17 August 2002, National University of Singapore, Singapore.

on the root surface in beagle dogs.<sup>8</sup> However, to the authors' knowledge, there have been no reports on scaffold-cell grafts harboring human PDLFs and alveolar osteoblasts (AOs) forming the PDL-bone interface. Critical-size defects involving multiple tissue types, such as the PDL and alveolar bone, require the application of scaffolds containing the appropriate cells for tissue development.<sup>9</sup> Consequently, transplantation of tissue-engineered grafts including scaffold-cell constructs appears to be a promising technique in regenerating periodontium.

A double construct of PDLF-seeded membrane and AO-seeded scaffold is hypothesized to have potential application in tissue engineering of periodontal structures. This paper reports the results of a 2-phase study of a novel membrane-scaffold graft construct to investigate its ability in supporting PDLF and AO attachment and growth *in vitro*, and its feasibility for tissue engineering a PDL-alveolar bone interface *in vivo*.

## MATERIALS AND METHODS

### Preparation of Membranes and Scaffolds

Membranes (mean thickness  $\pm$  SD,  $10 \pm 2 \mu\text{m}$ ) were fabricated from poly( $\epsilon$ -caprolactone) (PCL; Aldrich Chemical, Milwaukee, WI) by solution-casting and heat press, followed by biaxial stretching using an apparatus designed and built in-house.<sup>10</sup> Perforations approximately  $100 \mu\text{m}$  in diameter were created in biaxially-stretched membranes using a computer-guided desktop robot (Sony Robokids, Tokyo, Japan).<sup>11</sup> Membranes were treated by immersion in 5 mol/L sodium hydroxide (NaOH) for 3 hours with shaking at 140 rpm to increase hydrophilicity, rinsed extensively in distilled water, and sterilized with 70% ethanol and ultraviolet irradiation.<sup>11</sup> Thirty-four membranes,  $16 \times 16 \text{ mm}^2$ , were immersed in PDLF culture medium, ie, Dulbecco's Modified Eagle Medium (DMEM; Gibco-Life Technologies, Grand Island, NY) containing 10% fetal bovine serum (FBS), 4,500 mg/mL glucose, and 2% penicillin-streptomycin, at  $37^\circ\text{C}$  followed by overnight air drying. Subsequently, 30 membranes were sandwiched between custom-made 316L stainless steel O-rings (Alson Engineering, Singapore) (Fig 1a) for cell seeding. Four nonseeded membranes were set aside as negative controls.

Poly( $\epsilon$ -caprolactone) scaffolds with a lay-down pattern of 0/60/120 degrees and a porosity of approximately 65% were fabricated with a fused deposition modeling (FDM) 3D Modeller from Stratasys (Eden Prairie, MN).<sup>12</sup> The fully interconnected pores were approximately  $360 \times 430 \times 620 \mu\text{m}$ .<sup>12</sup> Scaffolds measuring  $8 \times 8 \times 5 \text{ mm}^3$  were treated with NaOH and sterilized using the method used for membranes.

Thirty-four scaffolds were immersed overnight in AO culture medium, ie, Medium199 (Gibco) containing 10% FBS and 2% penicillin-streptomycin at  $37^\circ\text{C}$  followed by overnight air drying. Four nonseeded scaffolds were set aside as negative controls.

### Seeding and Culture of PDLFs and AOs

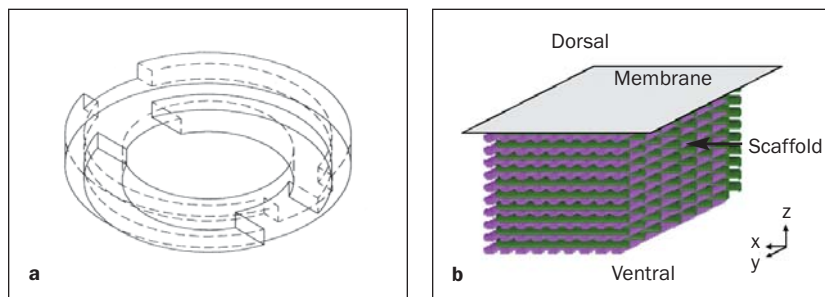
Human PDLF and AO explants were harvested<sup>13</sup> from a periodontally sound molar of a healthy 23-year-old female after informed consent was obtained according to the ethical guidelines of the Helsinki II declaration.<sup>14</sup> The study protocol was approved by the National University of Singapore Institutional Review Board. PDLFs between the fourth and fifth passages were seeded in 45-mL aliquots onto thirty sandwiched membranes at  $78,000 \text{ cells/cm}^2$ . Membrane-cell constructs were incubated at  $37^\circ\text{C}$  and 5%  $\text{CO}_2$  for 2 hours before DMEM was added.

Alveolar osteoblasts were mixed in a 1:2 (v/v) ratio according to the manufacturer's instructions with fibrin glue containing 70 to 110 mg/mL fibrinogen, 4 IU/mL thrombin, 40 mmol/L calcium chloride, and 3,000 kIU/mL of aprotinin (Tisseel Kit; Baxter, Vienna, Austria). Cell-fibrin mixtures in 55- $\mu\text{L}$  aliquots each were seeded at  $625,000 \text{ cells/cm}^3$  onto 30 scaffolds. Scaffold-cell constructs, encapsulated with 25  $\mu\text{L}$  of fibrin glue, were incubated for 30 minutes before Medium199 was added. Medium change was performed every 3 days for 3 weeks. All specimens were transferred to new wells at the end of each week. Encapsulation of the scaffold-cell constructs was repeated after 7 days to retain AOs in the scaffolds. Osteoinduction was carried out 14 days after seeding using medium supplemented with 50  $\mu\text{g/mL}$  ascorbic-2-phosphate, 10 mmol/L  $\beta$ -glycerophosphate, and  $10^{-7} \text{ mol/L}$  dexamethasone (Sigma, St Louis, MO).<sup>15</sup>

### In Vitro Characterization

Membrane-cell and scaffold-cell constructs were subjected to the following studies weekly for a period of 3 weeks. Morphological analysis was performed with phase contrast light microscopy (PCLM) (Olympus IX70, Tokyo, Japan) and scanning electron microscopy (SEM) (Jeol JSM-5600LV, Tokyo, Japan).<sup>15</sup> SEM specimens were gold-coated at 15 mA for 80 s and viewed under an accelerating voltage between 12 to 15 kV.

Cell viability assay was performed ( $n = 3$ ) with fluorescein diacetate (FDA) and propidium iodide (PI). Constructs were incubated with 2  $\mu\text{g/mL}$  FDA (Molecular Probes, Invitrogen, Carlsbad, CA) at  $37^\circ\text{C}$  at 5%  $\text{CO}_2$  for 15 minutes and with 0.1 mg/mL PI (Molecular Probes) for 3 minutes at room temperature, with rinsing after each step. Viewing was performed with a confocal laser scanning microscope (CLSM; Olympus IX-70 HLSH 100 Fluoview).



**Figs 1a and 1b** Three-dimensional representation of (a) a custom-made 316L stainless steel O-ring and (b) a membrane-scaffold construct with the implantation orientation indicated.

Metabolism was assayed separately ( $n = 3$ ) for cells retained on constructs and cells lost to the corresponding wells by CellTiter 96 AQ<sub>ueous</sub> One Solution Cell Proliferation Assay (Promega, WI). The substrate, 3-(4,5-dimethylthiazol-2-yl)-5-(3-carboxymethoxyphenyl)-2-(4-sulfophenyl)-2H-tetrazolium (MTS), was bioreduced into a brown formazan product by nicotinamide adenine dinucleotide phosphate (NADP) or its reduced form NADP hydrogen (NADPH) within living cells. Constructs were transferred to new wells weekly prior to assay. Five hundred microliters of assay reagents (1:5 MTS to culture medium ratio) were added per well. After 3 hours of incubation at 37°C and 5% CO<sub>2</sub>, 100- $\mu$ L aliquots of bioreduced mixture from each test well were transferred to a 96-well plate. Absorbance at 490 nm was determined.

Statistical analysis was carried out using the Student *t* test. Differences among samples were considered statistically significant when  $P < .05$ .

### Implantation

On the fourth week of culture, AO-containing scaffolds were paired with PDLF-containing membranes (experimental group,  $n = 9$ ), while the nonseeded scaffolds and membranes were paired in the control group ( $n = 4$ ). Scaffolds were trimmed at the edges, and assembly of fibrin glue-coated membrane-scaffold constructs (Fig 1b) was performed 1 hour prior to implantation to ensure adequate stability.

Subcutaneous implantation was performed in accordance with the International Guiding Principles for Animal Research<sup>16</sup> in a laminar flow hood under sterile conditions. Seven 12-week-old athymic Balb C mice (Animal Resources Centre, Murdoch, Australia) were anesthetized intraperitoneally with 0.15 mL of Dormicum (Roche, Basel, Switzerland) and Hypnorm (Janssen, Beerse, Belgium) mixed at a ratio of 1:1 (v/v). After disinfection with iodine and 70% alcohol, incisions approximately 10 mm long were made lateral to the dorsal spine to create bilateral subcutaneous pockets to accommodate 2 randomly selected constructs, inserted with the membrane facing dorsally. The mice were euthanized after 4 weeks. Both the constructs and surrounding soft tissues were harvested for evaluation.

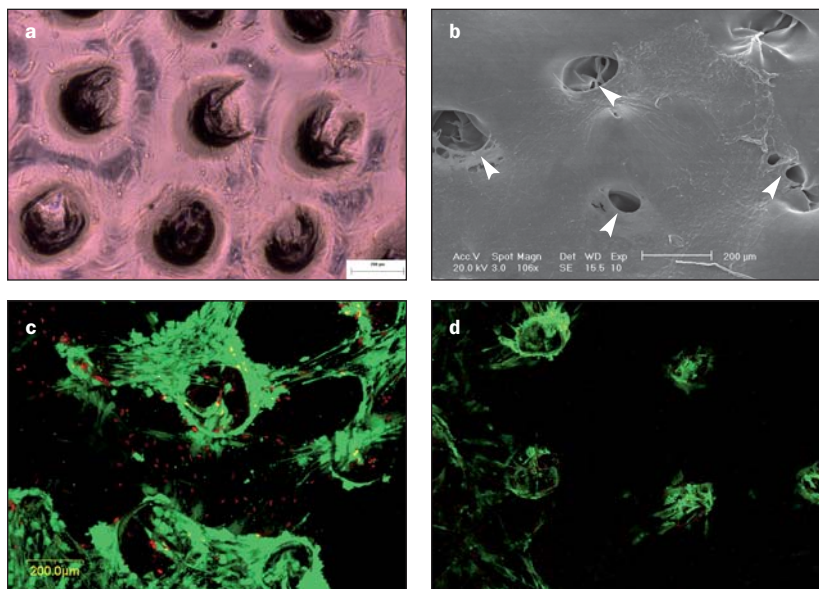
### Cryosectioning and Histology

Excised tissue blocks were cut into 2 diagonal halves, fixed in 4% formaldehyde in phosphate buffer solution (PBS) for 2 hours at room temperature, and immersed in 2 mol/L sucrose (Sigma) at 4°C overnight. One half of tissue blocks were embedded in tissue-freezing medium (H-TFM; Triangular Bio-medical Science, Durham, NC) and frozen by immersion in liquid nitrogen. Seven cryosections, 8 to 12  $\mu$ m in thickness, were made in the vertical “z” plane (Fig 1b). One cryosection each was stained with hematoxylin and eosin (H&E) and Masson’s trichrome, while the remaining 5 were processed for immunostaining. The other diagonal tissue block halves were embedded in polymethyl methacrylate, and 3 sections each were processed for Hale periodic acid-Schiff (PAS) and Giemsa staining.

### Immunohistochemical Analysis

Cryosections were processed with affinity purified polyclonal antibodies against major extracellular matrix (ECM) proteins present in PDLs and AOs to verify tissue identity, ie, type I collagen (1:200 dilution) (Biodesign, Saco, ME), type III collagen (1:40 dilution) (Chemicon, Temecula, CA), fibronectin (1:200 dilution) (Biodesign), vitronectin (1:20 dilution) (Santa Cruz Biotechnology, Santa Cruz, CA), and bone sialoprotein (BSP) (1:200 dilution) (Chemicon). Blocking was performed with 5% bovine serum albumin (w/v) and 1% goat serum (v/v) in PBS for 30 minutes at room temperature. Sections were incubated with primary antibodies overnight at 4°C in a humidified chamber. Incubation with secondary antibodies, anti-rabbit IgG-horseradish peroxidase (HRP) (R&D Systems, Minneapolis, MN), and anti-goat IgG-HRP (Chemicon) was performed according to manufacturer’s protocols (1:500 dilution). To distinguish between recipient and donor cells within the constructs, the former were identified by immuno-staining with antibodies against mouse-IgG-specific antibody (1:250 dilution) (Santa Cruz Biotechnology). Immunostaining for each antibody was performed on 3 randomly selected cryosections and counterstaining with hematoxylin was performed.

**Fig 2** Attachment, morphology, and viability of PDLFs on PCL membranes. (a) Uniform distribution of PDLFs was observed under PCLM at week 1, and (b) bridging of perforations was observed under SEM at week 2. Confocal laser microscopic image of PDLFs on (c) the top of the membrane and (d) the reverse side of membrane after FDA/PI staining at week 2. Note the clustering of cells around perforations and the migration of cells to the reverse side. White arrowheads indicate cell attachment and migration at sites of perforation.



## RESULTS

### In Vitro Characterizations

PDLFs attached uniformly on PCL membranes and appeared spindle-shaped at week 1 (Fig 2a). Cells were seen to migrate and bridge perforations, leading to confluent layers on the membranes at week 2 (Fig 2b). Under FDA/PI staining, the presence of viable attached PDLFs was observed throughout the in vitro culture (Fig 2c). In addition, cells were observed on the reverse sides of membranes (Fig 2d). However, the fluorescent signals on membranes disassembled from O-rings and rinsed during staining steps were frequently localized around perforations, with bridging between cell clusters (Fig 2c), as opposed to the relatively uniform coverage of attached PDLFs during culture (Fig 2a).

A majority of AOs were seen embedded in fibrin glue at week 1 postseeding. The initial onset of fibrinolysis was indicated by an increase in visibility of fibrin glue through the scaffold (Fig 3a). At week 2, increased cell density and fibrin degradation within scaffold pores were observed (Fig 3b). FDA/PI staining showed viable cell layers over the scaffold bars. The attached AOs on the scaffold bar appeared elongated, while those within the pores appeared to be stellate and bridged across the interconnected honeycomblike pores (Fig 3c). At week 3, AOs in scaffolds demonstrated positive von Kossa's staining (Fig 3d).

MTS assay over 3 weeks (Fig 4) showed a steep and steady increase in the metabolic rates of PDLFs on PCL membranes. AOs cultured on scaffolds showed a high metabolic rate in the first week, with a

gentler increase at weeks 2 and 3. There was a significant peak in the metabolic rates of PDLFs at the bottoms of culture wells at week 2 ( $P < .01$ ), whereas this was not distinct for AOs.

### In Vivo Characterizations of Constructs

The mice tolerated the surgical procedures well. Displacement of the membrane from the construct was observed in 4 specimens (2 each from experimental and control groups), and these were excluded from analysis. The final sample consisted of 7 specimens from the experimental group and 2 from the control group. There was a higher degree of vascular network infiltration and construct integration with recipient tissue in experimental group specimens. Tissue ingrowth through the membrane perforations at the membrane-scaffold interface was observed in the majority of specimens (Fig 5a). Hale-PAS and Giemsa staining gave uniform blue and pink coloration, respectively, representing musclelike tissue (Fig 5a) and fibrous and adipose tissue (Fig 5b). In contrast, control group specimens were characterized by predominant adipose tissue (Fig 5c) and the dissociation of the tissue-scaffold interface. Under Masson's trichrome staining, collagen was detected in dense fibrous tissue at the periphery of constructs (Fig 5d) and as parallel fibers along scaffold bars in the experimental group (Fig 5e). Inflammatory cell infiltration and degradation of PCL were not observed at week 4.

Immunostaining results for the major ECM proteins are summarized in Table 1. Negative controls in the absence of primary antibodies gave little or no staining. In accordance with the results of Masson's

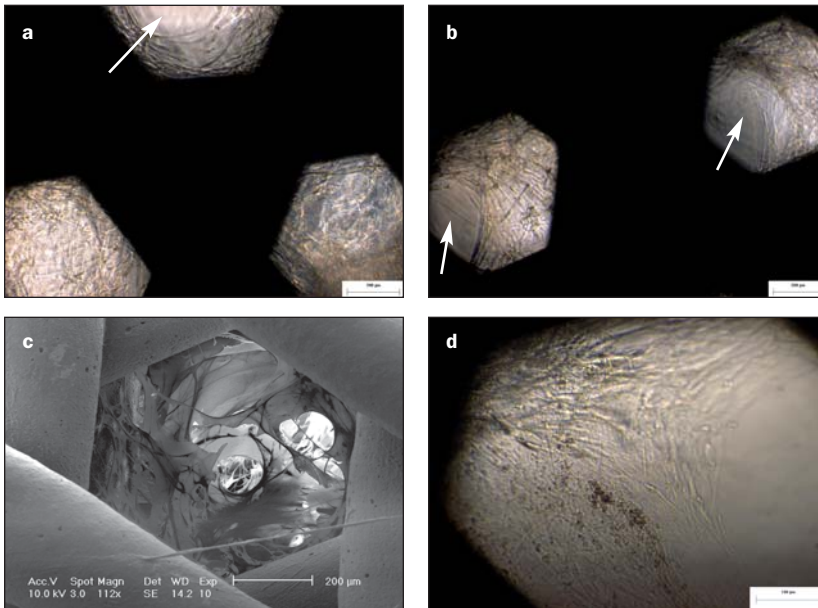


**Fig 3** Attachment, morphology, and viability of AOs on PCL scaffolds. AOs embedded in fibrin glue at (a) week 1 and (b) week 2. Signs of fibrin degradation were first observed at week 1, as indicated by an increase in visibility (white arrows). (c) AO attachment within scaffold pores under SEM. (d) Mineralized nodule formation (black arrow) was observed after osteoinduction at week 3 (von Kossa staining of osteoinduced AOs).

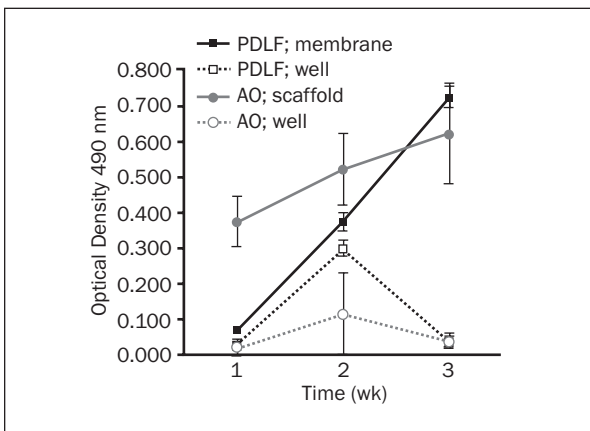


**Fig 4** Comparison of the metabolic activities (MTS assay) of PDLFs on membranes and of AOs on scaffolds, with their respective wells at weekly intervals.

trichrome staining (Fig 5e), type I collagen was observed to be present along the scaffold bars (Fig 6a), while the membrane-scaffold interface was positively stained for both collagen type III (Fig 6b) and type I (Fig 6c). Fibronectin was detected throughout the constructs, moderately at the tissue-scaffold interface and extensively at the periphery (Fig 6d). Vitronectin expression was localized only around the vasculature (Fig 6e). Staining for BSP gave negative results in all specimens examined. Immunostaining with anti-mouse IgG antibodies demonstrated the sites of recipient tissue within the constructs. The specificity of anti-mouse IgG antibody was verified by positive staining of mouse dermal sections (Fig 6f) and a lack of staining in human dermal fibroblasts (Fig 6g) and alveolar osteoblasts in vitro. Signals for anti-mouse IgG, detected mainly at the extra-

cellular ECM, were observed throughout constructs in control groups (Fig 6h) but mostly at the construct periphery and vasculature in experimental group (Figs 6i and 6j). PDL tissue was largely indistinguishable from surrounding fibrous connective tissues, except at areas of membrane-scaffold interface, where it was characterized by discrete cell layers and infiltration across perforated membranes (Fig 6j).

## DISCUSSION

This paper describes a novel concept for a PDL-alveolar bone graft construct. PCL, a bioresorbable scaffold polymer investigated for soft and hard tissue engineering,<sup>15,17-19</sup> was demonstrated in this study to support PDLF and AO attachment and growth

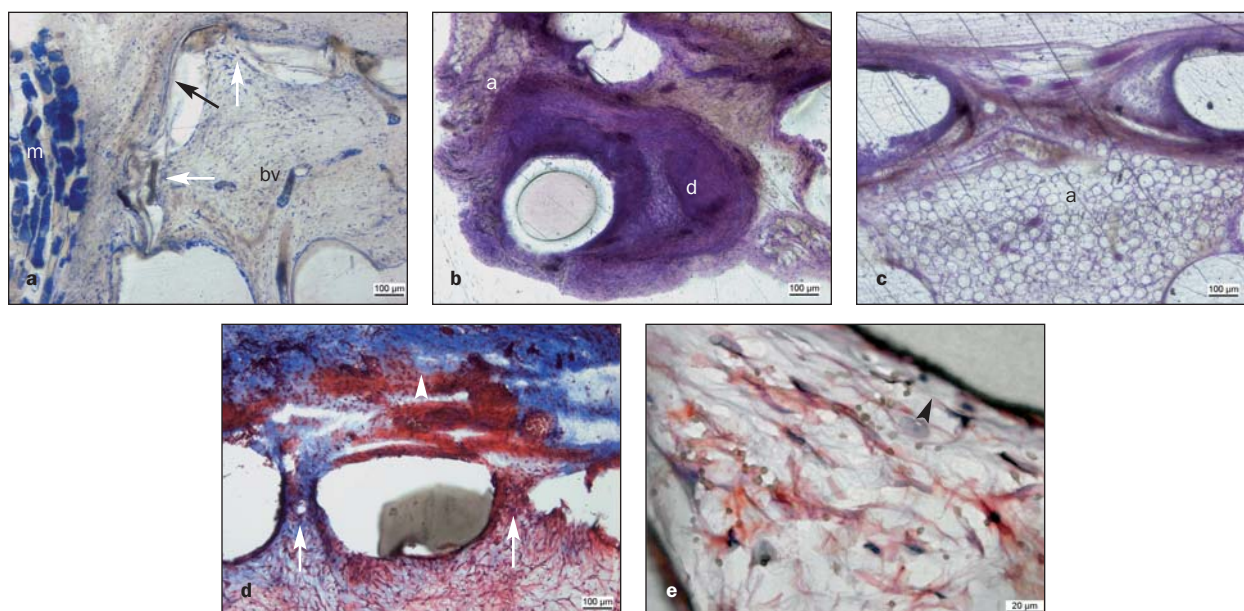


**Fig 5** Histologic analysis of constructs after 4 weeks in vivo. Representative morphology of constructs from experimental group after (a) Hale-PAS and (b) Giemsa staining. (c) Dislocation of PCL membrane and predominance of adipose tissue in a nonseeded control. Presence of collagen at (d) the periphery and (e) the tissue-scaffold interface under Masson's trichrome staining. a = adipose tissue; bv = blood vessel; d = dense fibrous tissue; m = musclelike; black arrow indicates PCL membrane; white arrows indicate tissue penetration across perforations; arrowheads indicate collagen fibers.

(Figs 2 and 3). Cells were highly proliferative on both membranes and scaffolds throughout the 3-week in vitro culture period (Fig 4). PDLFs proliferated on membranes and reached confluency at week 2 (Fig 2b), after which PDLFs continued to proliferate and migrate through perforations onto reverse sides (Fig 2d), enhancing the integration of the cell layers and the membrane. Cell detachment onto the bottom of culture wells was observed during rinsing after disassembly of O-rings (Fig 2c), possibly accounting for the peak in PDLF growth at the bottom of culture wells (Fig 4). The subsequent decrease in cell metabolism at week 3 was probably caused by a limitation in surface area for growth in wells.

Fibrin glue was employed during AO seeding as a carrier for the delivery of cells into scaffolds. Fibrin glue is biocompatible<sup>20</sup> and can be degraded by local fibrinolytic activity followed by the invasion of granulation tissue accompanied by macrophages<sup>21</sup> at about 1 week postinjury.<sup>2</sup> Components such as factor XIII and cross-linked fibrin were believed to stimulate cell proliferation and facilitate the formation of a fibroblast network via the clot structure in wound healing.<sup>22</sup> In this study, AOs within PCL scaffolds demonstrated a high metabolic rate in the first 2 weeks (Fig 4). The lengthened process of fibrinolysis, initiated at week 1 and extended until week 2, as suggested by the increase in visibility through the scaffold (Figs 3a and 3b), could be attributed to the

**Table 1** Summary of Immunostaining Results

Protein	Group	Membrane	Central tissue	Tissue-scaffold interface
Collagen I	E	-/+	-/+	-/+
	C	-/+	-/+	-/+
Collagen III	E	-/+	-/+	-/+
	C	-/+	-/+	-
Fibronectin	E	+	+	+
	C	+	+	+
Vitronectin	E	-/+*	-/+*	-
	C	-/+*	-/+*	-
BSP	E	-	-	-
	C	-	-	-
Mouse IgG	E	+	-/+	-/+
	C	+	+	+

E = experimental; C = control; - = absent; + = present.

\*Staining localized at blood vessels.

action of aprotinin from fibrin glue used during seeding and encapsulation. Aprotinin has been shown to negatively regulate plasmin<sup>23</sup> and hence slow down fibrin degradation. As cell proliferation and migration took place, AOs gradually emerged from the fibrin matrix and established contacts with

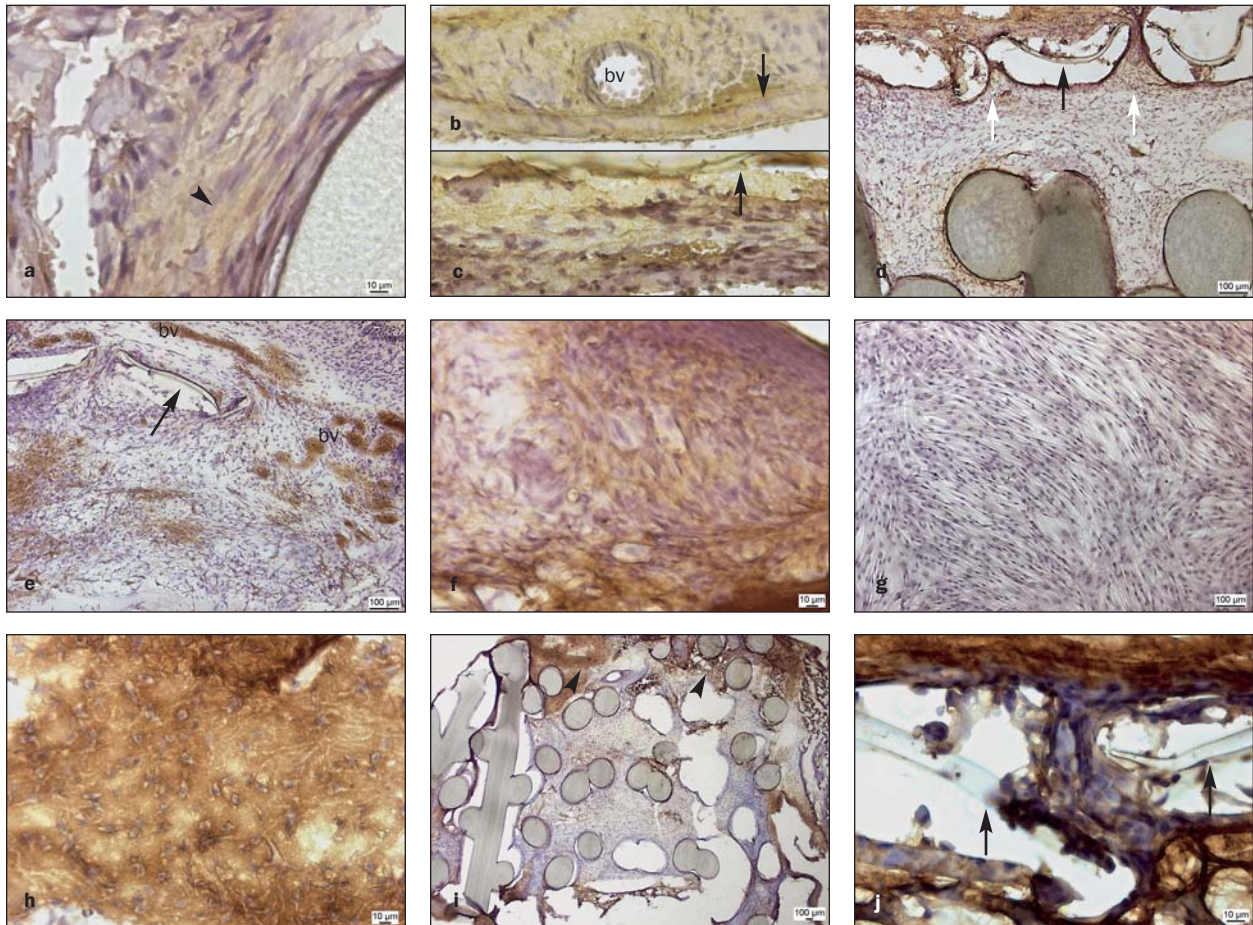


**Fig 6** Immunohistochemical analysis of constructs after 4 weeks in vivo. Sites of antigen localization are indicated by brown coloration, generated by the enzymatic conversion of 3,3'-diaminobenzidine (DAB) into brown precipitate by HRP. (a) Expression of type I collagen at tissue-scaffold interface, as indicated by brown coloration. Expression of (b) type III and (c) type I collagen at membrane. Note the differing tissue morphology at (b) the construct periphery and (c) the membrane-scaffold interface. (d) Expression of fibronectin, strong at periphery and moderate at tissue-scaffold interface. (e) Expression of vitronectin near vasculature. Immunostaining of anti-mouse IgG in (f) nude mice dermal sections (positive control) and (g) human dermal fibroblasts (negative control). Expression of anti-mouse IgG in (h) the control and (i and j) experimental groups. Cells of mouse origin (black arrowheads) were found mainly at the periphery and areas of vascularization. (j) Close-up image at the membrane-scaffold interface, showing the infiltration of putative PDLF cell-sheet through the perforation. bv = blood vessel; black arrows indicate PCL membrane; white arrows indicate tissue penetration across perforations (immunohistochemical stain [DAB substrate]; counterstained with hematoxylin).

the PCL surface via focal adhesion points.<sup>15</sup> AOs embedded in fibrin glue but unattached to PCL were lost with fibrinolysis onto the bottom of culture wells (Fig 4). Mineralized nodule formation, characterized by cell aggregates and positive von Kossa staining, was observed at week 3 (Fig 3d), which is in accordance with previously reported *in vitro* studies on bone engineering.<sup>15</sup>

Histochemical examination of *in vivo* constructs in the experimental group after 4 weeks demonstrated highly vascularized tissue, including ingrowth of muscle, fibrous, and adipose tissues from the recipient (Figs 5a to 5c). This incidentally also provided evidence for the advantages of a scaffold with high porosity with respect to nutrient supply which is a determining factor for the survival, proliferation, and

differentiation of transplanted cells.<sup>24</sup> Connective tissue invasion, identified by immunostaining with anti-mouse IgG antibodies, was detected mainly at the construct periphery and vasculature. Cells within constructs secreted ECM, observed as collagen fibers aligning along scaffold bars (Fig 5e), whereas cells at the membrane-scaffold interface secreted collagen, which was deposited between cell layers. Fibronectin and vitronectin, usually found in newly-formed PDL and osteoid at 4 and 8 weeks postinjury,<sup>25</sup> were also detected in the constructs. Unlike the ubiquitous distribution of fibronectin, vitronectin was expressed only by cells near the vasculature, in accordance with its presence in plasma, platelet  $\alpha$ -granules, and vessel walls.<sup>26</sup> On the other hand, cell penetration through the 100- $\mu$ m-diameter membrane perfora-

tions allowed for enhanced integration with the scaffolds (Figs 5a and 5d). Despite this, membrane displacement was observed because of a lack of physical interlocking of the membrane and scaffold. However, the loss of construct integrity at the membrane-scaffold interface and the weakened bonding of tissue-to-scaffold bars were more pronounced in nonseeded controls, which demonstrates the crucial role of seeded cells in scaffold-cell constructs.

The observation of increased ECM and mineralized nodule formation of AOs after week 2 *in vitro* (Figs 3c and 3d) was in accordance with earlier findings.<sup>27</sup> A similar experiment involving the subcutaneous implantation of human periosteum-derived osteoprogenitor cells on PCL scaffold reported bone formation.<sup>15</sup> Furthermore, recent studies have demonstrated the ability of AOs to express osteogenic proteins such as osteopontin and osteocalcin on PCL scaffolds (unpublished data, 2005). In contrast, no mineralization was found within the *in vivo* constructs. BSP, a mineralized tissue-specific marker with an established role in bone calcification,<sup>28</sup> was not detected within the constructs, which may be suggestive of a loss of phenotypic differentiation. Inhibition of osteogenesis via the release of prostaglandins by PDLFs has previously been reported.<sup>29</sup> Given that the PDL has been associated with root resorption due to prostaglandin E2 production by PDLFs,<sup>30</sup> and that prostaglandins stimulate bone resorption in long-term organ culture,<sup>31</sup> it may be speculated that the interaction between PDLFs and AOs interfered with the osteogenesis of AOs at the interface of soft and mineralizing tissues. In addition, for tissue-engineered constructs, cellular responses at the recipient site can strongly affect tissue formation.<sup>24</sup> Macroencapsulation of cell transplants has been proposed as a means to protect maturing mesenchymal tissue from the *in vivo* environment.<sup>32</sup> This needs to be investigated further in future studies.

In conclusion, both matrices supported PDLF and AO attachment and proliferation *in vitro*. The membrane-scaffold construct facilitated tissue growth and vascularization while providing strength and form *in vivo*.

## ACKNOWLEDGMENTS

This study was supported by a Faculty Research Grant (R-224-000-011-112) from the Faculty of Dentistry, National University of Singapore. The authors acknowledge the kind donation of PCL scaffolds by Singapore Temasek Polytechnic, fibrin glue by Dr Katharina Bittner (Baxter, Hyland Immuno, Austria), and technical assistance by Dr J.T. Schantz and Yefang Zhou.

## REFERENCES

1. Sae-Lim V, Ong WY, Li Z, Neo J. The effect of basic fibroblast growth factor on delayed-replanted monkey teeth. *J Periodontol* 2004;75:1570–1578.
2. Amar S. Implications of cellular and molecular biology advances in periodontal regeneration. *Anat Rec* 1996;245:361–373.
3. Sae-Lim V. Repair or regeneration of damaged dental structures—A dental trauma model. *Lifeline* (National University Hospital, Singapore) 2001;(Dec):7–8.
4. Bartold PM, McCulloch CAG, Narayanan AS, Pitaru S. Tissue engineering: A new paradigm for periodontal regeneration based on molecular and cell biology. *Periodontol* 2000 2000;24:253–269.
5. Quteish D, Singrao S, Dolby AE. Light and electron microscopic evaluation of biocompatibility, resorption and penetration characteristics of human collagen graft material. *J Clin Periodontol* 1991;18:305–311.
6. Grzesik WJ, Kuzentsov SA, Uzawa K, Mankani M, Robey PG, Yamauchi M. Normal human cementum-derived cells: Isolation, clonal expansion, and *in vitro* and *in vivo* characterization. *J Bone Miner Res* 1998;13:1547–1554.
7. Prato GP, Rotundo R, Magnani C, Soranzo C, Muzzi L, Cairo F. An autologous cell hyaluronic acid graft technique for gingival augmentation: A case series. *J Periodontol* 2003;74:262–267.
8. Nakahara T, Nakamura T, Kobayashi E, et al. *In situ* tissue engineering of periodontal tissues by seeding with periodontal ligament-derived cells. *Tissue Eng* 2004;10:537–544.
9. Murphy WL, Mooney DJ. Controlled delivery of inductive proteins, plasmid DNA and cells from tissue engineering matrices. *J Periodontol Res* 1999;34:413–419.
10. Ng CS, Teoh SH, Chung TS, Hutmacher DW. Simultaneous biaxial drawing of poly( $\epsilon$ -caprolactone) films. *Polymer* 2000;41:5855–5864.
11. Htay AS, Teoh SH, Hutmacher DW. Development of perforated microthin poly( $\epsilon$ -caprolactone) films as matrices for membrane tissue engineering. *J Biomater Sci Polym Ed* 2004;15:683–700.
12. Hutmacher DW, Schantz JT, Zein I, Ng KW, Teoh SH, Tan KC. Mechanical properties and cell cultural response of polycaprolactone scaffolds designed and fabricated via fused deposition modelling. *J Biomed Mater Res* 2001;55:203–216.
13. Chou AM, Sae-Lim V, Lim TM, et al. Culturing and characterization of human periodontal ligament fibroblasts—A preliminary study. *Mater Sci Eng C* 2002;20:77–83.
14. World Medical Association Declaration of Helsinki: Ethical principles for medical research involving human subjects. *JAMA* 2000;284:3043–3045.
15. Schantz JT, Hutmacher DW, Chim H, Ng KW, Lim TC, Teoh SH. Induction of ectopic bone formation by using human periosteal cells in combination with a novel scaffold technology. *Cell Transplant* 2002;11:125–138.
16. Howard-Jones N. A CIOMS ethical code for animal experimentation. *WHO Chron* 1985;39:51–56.
17. Ng KW, Hutmacher DW, Schantz JT, et al. Evaluation of ultra-thin poly( $\epsilon$ -caprolactone) films for tissue-engineered skin. *Tissue Eng* 2001;7:441–455.
18. Li WJ, Danielson KG, Alexander PG, Tuan RS. Biological response of chondrocytes cultured in three-dimensional nanofibrous poly( $\epsilon$ -caprolactone) scaffolds. *J Biomed Mater Res* 2003;67A:1105–1114.
19. Williamson MR, Coombes AG. Gravity spinning of polycaprolactone fibres for applications in tissue engineering. *Biomaterials* 2004;25:459–465.

20. Romanos GE, Strub JR. Effect of Tissucol on connective tissue matrix during wound healing: An immunohistochemical study in rat skin. *J Biomed Mater Res* 1998;39:462–468.
21. Warrer K, Karring T. Effect of Tisseel on healing after periodontal flap surgery. *J Clin Periodontol* 1992;19:449–454.
22. Redl H, Schlag G, Dinges P. The use and biocompatibility of a human fibrin sealant for hemostasis and tissue sealing. In: Williams DF (ed). *Biocompatibility of Tissue Analogs*, vol 1. Boca Raton, FL: CRC, 1985:150–153.
23. de Haan J, van Oeveren W. Platelets and soluble fibrin promote plasminogen activation causing downregulation of platelet glycoprotein Ib/IX complexes: Protection by aprotinin. *Thromb Res* 1998;92:171–179.
24. Muschler GF, Nakamoto C, Griffith LG. Engineering principles of clinical cell-based tissue engineering. *J Bone Joint Surg Am* 2004;86A:1541–1558.
25. Matsuura M, Herr Y, Han KY, Lin WL, Genco RJ, Cho MI. Immunohistochemical expression of extracellular matrix components of normal and healing periodontal tissues in the beagle dog. *J Periodontol* 1995;66:579–593 [erratum 1995;66:905–914].
26. Jang YC, Arumugam S, Ferguson M, Gibran NS, Isik FF. Changes in matrix composition during the growth and regression of human hemangiomas. *J Surg Res* 1998;80:9–15.
27. Franceschi RT. The developmental control of osteoblast-specific gene expression: Role of specific transcription factors and the extracellular matrix environment. *Crit Rev Oral Biol Med* 1999;10:40–57.
28. Boskey A. Matrix proteins and mineralization: An overview. *Connect Tissue Res* 1996;35:357–363.
29. Ogiso B, Hughes FJ, Davies JE, McCulloch CAG. Fibroblastic regulation of osteoblast function by prostaglandins. *Cell Signal* 1992;4:627–639.
30. Shiraishi C, Hara Y, Abe Y, Ukai T, Kato I. A histopathological study of the role of periodontal ligament tissue in root resorption in the rat. *Arch Oral Biol* 2001;46:99–107.
31. Nefussi JR, Baron R. PGE2 stimulates both resorption and formation of bone in vitro: Differential responses of the periosteum and the endosteum in fetal rat long bone cultures. *Anat Rec* 1985;211:9–16.
32. Haisch A, Groger A, Radke C, et al. Macroencapsulation of human cartilage implants: Pilot study with polyelectrolyte complex membrane encapsulation. *Biomaterials* 2000;21:1561–1566.